Published in final edited form as:
Mol Cancer Ther. 2011 April ; 10(4): 679–686. doi:10.1158/1535-7163.MCT-10-0833.

Rapamycin reverses splenomegaly and inhibits tumor development in a transgenic model of Epstein-Barr Virus-related Burkitt's lymphoma

Osman Cen and **Richard Longnecker**
Department of Microbiology and Immunology, Feinberg School of Medicine, Northwestern University, Chicago, IL

Abstract

Epstein-Barr virus (EBV) infection and latency has been associated with malignancies including nasopharyngeal carcinoma and Burkitt's lymphoma. EBV encoded latent membrane protein 2A (LMP2A) is expressed in most EBV-associated malignancies and as such provides a therapeutic target. Burkitt's lymphoma is a hematopoietic cancer associated with the translocation of c-MYC to one of the immunoglobulin gene promoters leading to abnormally high expression of MYC and development of lymphoma. Our laboratory has developed a murine model of EBV-associated Burkitt's lymphoma by crossing LMP2A transgenic mice with MYC transgenic mice. Since LMP2A has been shown to activate PI3K/Akt/mTOR pathway, we tested the therapeutic efficacy of mTOR inhibitor rapamycin on the tumors and splenomegaly in this double transgenic mice (Tg6/λ-MYC). We found that rapamycin reversed splenomegaly in Tg6/λ-MYC mice prior to tumor formation by targeting B cells. In a tumor transfer model, we also found that rapamycin significantly decreased tumor growth, splenomegaly, and metastasis of tumor cells into bone marrow of tumor recipients. Our data show that rapamycin may be a valuable candidate for the development of a treatment modality for EBV positive lymphomas such as Burkitt's lymphoma, and more importantly, provides a basis to develop inhibitors that specifically target viral gene function in tumor cells that depend on LMP2A signaling for survival and/or growth.

Keywords

EBV; LMP2A; Burkitt's lymphoma; tumor; splenomegaly; rapamycin

Background

Epstein-Barr virus (EBV) is a ubiquitous virus infecting oral epithelial cells and B-lymphocyte (1). Infection in early childhood typically leads to an asymptomatic infection whereas infection in adolescence or adulthood can result in infectious mononucleosis (2). Primary infection is mostly cleared by a T cell response, but a latent infection is established in a very few infected B cells (1). EBV latency has been associated with malignant diseases including nasopharyngeal carcinoma, Hodgkin's lymphoma, Burkitt's lymphoma, and post transplant lymphoproliferative disorders (PTLD) (1). In addition, HIV/AIDS patients are particularly susceptible to EBV-related malignancies. Latent membrane protein 2A

Corresponding Author: Richard Longnecker (or Osman Cen), Department of Microbiology and Immunology, Feinberg School of Medicine, Northwestern University, 303 E. Chicago Ave, Ward 6-241, Chicago IL 60611, Phone: 312 503-1354, Fax: 312-503-34722, r-longnecker@northwestern.edu (or o-cen@northwestern.edu)..

Conflicts of Interest: The authors disclose no conflicts of interest.

(LMP2A) is an EBV encoded protein that functions as a B cell receptor (BCR) mimic (3-5). It contains WW motifs, which mediate association with Nedd4 family ubiquitin ligases, resulting in degradation of cellular proteins (6-9). LMP2A also contains an immunoreceptor tyrosine-based activation motif (ITAM) that the Syk tyrosine kinase binds and a related phosphotyrosine motif that the Lyn kinase binds (3,10,11). As a result, LMP2A induces a BCR-like signal even in the absence of a functional BCR (3,5). Finally, studies have shown that LMP2A is expressed in primary Burkitt's lymphoma biopsies using a combination of quantitative RT-PCR and Western Blotting (12-15).

Burkitt's lymphoma is a hematopoietic cancer associated with the translocation of c-MYC to one of the immunoglobulin gene promoters leading to abnormally high expression of MYC and development of lymphoma (16). Transgenic expression of MYC in mice leads to lymphoma development (17,18). Our laboratory has developed a model of EBV-associated Burkitt's lymphoma (Tg6/λ-MYC) by crossing LMP2A transgenic mice (Tg6) with MYC transgenic mice (λ-MYC) (4,5,17,19). The Tg6/λ-MYC mice develop lymphoma around six-weeks of age whereas the λ-MYC mice typically take greater than 25 weeks to develop lymphoma (19,20).

The activation of PI3K/Akt/mTOR pathway has been observed in many EBV-associated disorders (21). Earlier studies have shown that Akt is a downstream target of LMP2A in B cells (22-25). LMP2A expression induces PI3K-dependent AKT phosphorylation (22,26) and activation of rapamycin-sensitive mTOR pathway (27). Rapamycin inhibits cell growth and modulates the cell cycle of EBV-positive lymphomas *in vitro* (27,28). Therefore, we tested the effect of mTOR inhibitor rapamycin on the splenomegaly and tumor development in the Tg6/λ-MYC mice. We found that rapamycin reversed spleen enlargement (splenomegaly) and decreased tumor size in both pre-tumor and lymphoma transfer models indicating that rapamycin blocks LMP2A activated pathways that promote cell survival and tumor development.

Materials and Methods

Animals

All animal experiments were conducted in the animal facility of the Center for Comparative Medicine at the Northwestern University following Institutional Animal Care and Use Committee (IACUC) guidelines. Wild type C57BL/6 and Rag1 KO (B6.129S7-Rag1^{tmMom}/J, catalogue no 002216) mice were purchased from Jackson Laboratories (ME). The MYC transgenic (λ-myc) and LMP2A – MYC double transgenic (Tg6/λ-MYC) mice have previously been described (5,17,19,29).

Tumor transfer model

Cervical or peripheral lymph node tumors were harvested from λ-MYC or Tg6/λ-MYC mice, processed into single cells, and either immediately used or aliquoted and frozen at 140°C. For tumor transfer, the freshly isolated or thawed 1×10^6 λ-MYC or Tg6/λ-MYC lymphoma cells were subcutaneously implanted into the right flank of anesthetized Rag1 KO mice which developed local tumors in 2-3 weeks.

Rapamycin treatment

Rapamycin (LC laboratories, MA) was dissolved in DMSO at 45 mg/ml, aliquoted, and kept at −20°C during the study. On the treatment day, the aliquots were diluted with 5.1% polyethylene glycol (PEG-400) (EMD, Fisher, PA) and 5.1% tween-80 (Fisher, PA) immediately before use as previously reported (30). In both pre-tumor and tumor transfer models (when tumors were palpable), the animals received 5-mg/kg rapamycin or equivalent

amount of DMSO as intra-peritoneal injections daily for 10 days. On the day 11, the animals were sacrificed; tumor, spleen, and bone marrow were harvested, documented, and analyzed with flow-cytometry. In the pre-tumor model, the mice were 5 to 9 weeks old when the treatment was started; the data are from one of three separate experiments and each data point is from 2-6 mice. In the tumor transfer model, mice were 8 to 15 weeks old at the time of tumor-cell transfer. The data shown are from one of two separate experiments. Each data point is from 3-5 mice.

Flow cytometry

The harvested tumors, spleens, or bone marrow were processed into single cells. One million cells were stained with specific antibodies, acquired with FacsCantoII (BD biosciences, CA) at the Northwestern University ImmunoBiology Flow Cytometry Core Facility. The following antibodies were used to stain the cells: B220-V450, CD19-FITC, IgM-PE, 7-AAD, Annexin V-APC (BD Biosciences, CA), and CD3 (eBioscience, CA). The data were analyzed with FlowJo software (Tree Star, OR). Unless otherwise indicated, the following sequential gating was performed for analysis: live cells (7AAD negative), singlet, lymphocyte, and population of interest.

Statistical analysis

The data were analyzed with unpaired two-tailed T test using GraphPad Prism (GraphPad Software Inc, CA). Data were graphed in a box-and-whisker format. The box for each group represents the interquartile range (25-75 percentiles) and the longer line in the box is the median value. The mean is indicated by + sign, which may be seen as a short line when it coincides with a vertical line or absent when the median and mean correspond. The whiskers indicate minimum and maximum data points. Note that when there are fewer than four data points in a group, a vertical line is shown and not a box. The p value of 0.05 and below was considered statistically significant.

Results

Rapamycin reverses splenomegaly in Tg6/λ-MYC mice

To determine if rapamycin treatment inhibits LMP2A induced splenomegaly, wild type, λ-MYC, or Tg6/λ-MYC mice were treated daily with 5-mg/kg rapamycin or equivalent amount of DMSO for 10 days. While rapamycin treatment did not significantly alter the size of the spleen in either wild type or λ-MYC mice, it decreased the spleen size in Tg6/λ-MYC mice nearly to that of wild type (Figures 1A and 1B). The average spleen weight in the DMSO group was 697 (SEM=0.074) milligrams while it was 160 (SEM=0.022) milligrams in the rapamycin treated Tg6/λ-MYC group. This corresponds to a 77% decrease (p value of 0.0005) (Figure 1B). The decreased spleen size correlated with a dramatic decrease in the percentage of B cells staining for the pan B cell marker B220 in the bone marrow and spleen of the treated animals (Figure 1C). Even though, rapamycin decreased the percentage of bone marrow B220 positive cells in wild type (from 36% to 18%) and λ-MYC mice (from 39% to 12%), the decrease in Tg6/λ-MYC was more than six fold (from 77% to 12%) (Figure 1C, left panel). In the spleen, rapamycin decreased the percentage of B220 positive cells from 80% to 35% in Tg6/λ-MYC while this decrease was from 47% to 24% in λ-MYC, and no change in the wild type (46% vs. 48%) was noticed (Figure 1C, right panel). We also observed that the decrease in the percentage of B220 positive cells correlated with an increase in the number of T cells using the pan T cell marker CD3 in the spleen of Tg6/λ-MYC mice (Figure 1D). Normally, untreated Tg6/λ-MYC mice, at an early age, have a dramatic decrease in the CD3 positive population in the spleen. After tumor development, this number further decreases to below 1% (data not shown). Rapamycin treatment increased the CD3 positive cell population from 0.7% to 25% nearly to that of wild type. The

percentage of CD3 population in wild type or λ-MYC did not change with rapamycin treatment (Figure 1D).

Tg6/λ-MYC lymphoma cells form tumors in recipient Rag1 KO mice

To test the effect of candidate therapeutic compounds that may specifically target Tg6/MYC lymphomas, we established a tumor transfer model, in which we implanted 1×10^6 λ-MYC or Tg6/λ-MYC lymphoma cells subcutaneously into the right flank of Rag1 deficient (Rag1 KO) mice and observed for tumor development. The kinetics of secondary tumor development was very similar in the recipients and tumors developed in both groups within three weeks after the cell transfer (data not shown).

Rapamycin decreases Tg6/λ-MYC tumor mass in recipient Rag1 KO mice

To test the effect of the rapamycin on LMP2A-associated tumor development, we treated recipient mice in our tumor transfer model with rapamycin after tumors were palpable. Rapamycin treatment significantly inhibited tumor development as well as splenomegaly in Tg6/λ-MYC tumor recipients (Figure 2). The tumor mass was significantly reduced in recipients of both Tg6/λ-MYC and λ-MYC tumors after rapamycin treatment; however, this decrease was much more pronounced in the recipients of Tg6/λ-MYC tumor cells than in those that received λ-MYC tumor cells (Figures 2A and 2C). In mice receiving Tg6/λ-MYC lymphoma cells, the average tumor mass was 5.09 (SEM=0.508) grams in the DMSO control group while it was 1.04 (SEM=0.229) grams in the rapamycin-treated group (Figure 2C). This decrease corresponds to an 80% reduction (p=0.0001). The rapamycin-induced decrease in the tumor size was less pronounced in mice receiving λ-MYC lymphoma cells (Figures 2A and 2C). The tumor size in the λ-MYC lymphoma recipients was 2.25 (SEM=0.46) grams in the DMSO group and 0.94 (SEM=0.27) grams in the rapamycin-treated group (Figure 2C). This decrease corresponds to a 58% inhibition (p=0.0476). We also observed that the Tg6/λ-MYC tumors generally grew to a larger size than λ–MYC tumors in the recipients (Figure 2A and 2C), which may be attributed to proliferation and survival signals induced by LMP2A and reflective of the much more rapid onset of these tumors when compared to the λ-MYC tumors.

Rapamycin decreases Tg6/λ-MYC-induced splenomegaly in recipient Rag1 KO mice

In our tumor transfer model, despite the fact that the tumor is implanted subcutaneously into the right flank of the mice, the tumor cells metastasize into other organs including bone marrow and spleen. One result of this dissemination is the development of splenomegaly in the recipients. With the rapamycin treatment, we observed a significant decrease in the splenomegaly only in Tg6/λ-MYC tumor recipients (Figures 2B and 2D). In the mice receiving Tg6/λ-MYC lymphoma cells, the average spleen mass was 413 milligrams in the DMSO control group while it was 208 milligrams in the rapamycin group (Figure 2D). This decrease corresponds to a 50% inhibition of splenomegaly (p 0.0041). In the λ-MYC tumor recipients, there was no significant difference between the two groups (Figure 2D). The spleen size in the λ-MYC lymphoma recipients was 677 milligrams in the DMSO group and 635 milligrams in the rapamycin group (Figure 2D). This corresponds only to a 6% inhibition (p 0.819). In addition, we also observed that the spleens in recipients of Tg6/λ-MYC lymphoma cells were generally smaller than those of mice that received λ–MYC lymphoma cells (Figures 2B and 2D).

Rapamycin decreases metastasis of Tg6/λ-MYC lymphoma cells into the bone marrow of recipient Rag1 KO mice

In preliminary experiments, we had observed that the transferred lymphoma cells repopulated the recipient bone marrow. To assess whether rapamycin treatment was also

effective in decreasing the metastases of lymphoma cells, we tested for B cells using the pan B cell marker CD19 in the bone marrow of recipient mice. Rag1 KO mice do not have mature B cells (31). In the naïve Rag1 KO, we detected a small number (3%) of CD19 positive cells in the bone marrow, which may correspond to early B cell progenitors. In wild type mice, approximately 30% of the cells were CD19 positive B cells. In the tumor-transferred Rag1 KO mice, however, we observed a very high percentage of CD19 positive cells in the bone marrow. The increased percentage of CD19 positive bone marrow cells is indicative of metastasis of transferred lymphoma cells into the bone marrow. In rapamycin-treated group, the percentage of CD19 positive cells in the bone marrow significantly decreased in the Tg6/λ-MYC group (Figure 3, left panel). The percentage of CD19 positive cells in the bone marrow of Tg6/λ-MYC recipients was 45% and 18% in DMSO and rapamycin groups, respectively. This corresponds to a 60% decrease (p 0.012). Even though there was a considerable decrease in the percentage of CD19 positive cells in the bone marrow of λ-MYC tumor recipients treated with rapamycin, this difference did not reach statistical significance. The percentages of CD19 positive cells in the bone marrow of λ-MYC recipients were 68% and 42% in DMSO and rapamycin groups, respectively (Figure 3, left panel). This corresponds to a 38% decrease (p 0.209).

As in the bone marrow, there were only a few percent, if any, CD19 positive cells in the spleen of naïve Rag1 KO mice. However, in the spleen of lymphoma recipients, more than 70% of splenocytes were CD19 positive. After rapamycin treatment, we observed a slight decrease in the percentage of CD19 positive cells in the spleens of both groups (Figure 3, middle panel). In the Tg6/λ-MYC recipients, the average percentage of CD19 positive cells in the spleen was 78% and 70% in DMSO and rapamycin groups, respectively. Similarly, in the recipients of λ-MYC lymphoma cells, the corresponding values were 90% and 81% in DMSO and rapamycin groups, respectively.

Almost all the tumor cells (92%-99%) in recipients of both Tg6/λ-MYC and λ-MYC lymphoma cells were CD19 positive (Figure 3, right panel). Rapamycin treatment caused a slight but statistically significant decrease in CD19 positive cells in the tumors of Tg6/λ-MYC lymphoma recipients (from 99% to 95%, p 0.030). The decrease in the corresponding CD19 positive values in the λ-MYC lymphoma recipients however was not significant (from 97% to 96%, p 0.553). In addition, the percentages of CD19 positive cells in the bone marrow and spleen, but not in the tumor, of the λ-MYC tumor recipients were slightly higher than those of Tg6/λ-MYC recipients (Figure 3).

Rapamycin induces apoptosis of Tg6/λ-MYC lymphoma cells in the spleen of recipients

To assess whether the decrease in the tumor size and splenomegaly correlated with increased cell death, we measured apoptosis by annexin V staining. Figure 4A shows annexin V staining of live cells (7AAD negative) in representative samples from DMSO or rapamycin groups of Tg6/λ-MYC and λ-MYC lymphoma recipients. Overall, The rapamycin treatment caused an increase in apoptosis in total live splenocytes and tumor cells (data not shown). To assess the specific effect of rapamycin on tumor cells, we then analyzed the percentage of annexin V positive cells on live-CD19 positive gated cells (Figure 4B). In the recipients of Tg6/λ-MYC lymphoma cells, we noticed a significant increase in the level of apoptosis in CD19 positive cells from the spleen (Figure 4B, middle panel, from 18% to 27%, p 0.022) but a significant decrease in apoptosis in the bone marrow CD19 positive cells (Figure 4B, left panel, from 17% to 10%, p 0.015) in the same recipients. In the tumors of Tg6/λ-MYC recipients treated with rapamycin, there was highly variable annexin V staining and despite the higher mean value of apoptosis (4.7% vs. 12.8%), the level did not reach statistical significance (Figure 4B, right panel). In the recipients of λ-MYC lymphoma cells, there was no significant change in the apoptosis level in spleen, bone marrow, or tumor cells with rapamycin treatment (Figure 4B).

Discussion

Our data show that rapamycin significantly interferes with the LMP2A-induced survival signaling in our transgenic Tg6/λ-MYC model of Burkitt's lymphoma. Indicative of the sensitivity of Tg6/λ-MYC cells to rapamycin, we observed a dramatic reduction in spleen size and a restoration of normal splenic T and B cell populations when Tg6/λ-MYC mice were treated prior to tumor development (Figure 1). This dramatic difference was not observed in control λ-MYC or WT mice. In our tumor transfer model, Tg6/λ-MYC tumors were very sensitive to rapamycin treatment (Figure 2 and 3). We did observe a modest effect on λ-Myc tumors with rapamycin treatment, but this effect was not of statistical significance in contrast to Tg6/λ-Myc tumors. Interestingly, despite the limited sensitivity of λ-Myc tumors to rapamycin, splenomegaly was not reversed by rapamycin following λ-Myc tumor transfer in contrast to whenTg6/λ-Myc tumor cells were transferred. The nature of this difference is not clear, but it may be related to additional changes or the splenic microenvironment that may render λ-Myc tumors less dependent on the mTOR pathway when the tumor has metastized to the spleen.

We also observed increased apoptosis in Tg6/λ-myc tumor cells when compared with λ-MYC tumor cells (Figure 4) which may be related to our previous observation that the p53 pathway is still active in the Tg6/λ-MYC tumors in contrast to the λ-MYC tumors which harbor p53 pathway mutations (19,32). The absence of p53 pathway mutations in the Tg6/λ-MYC tumors may result in tumor cells more susceptible to apoptotic signals such as treatment with rapamycin when compared with λ-MYC tumors.

Related to apoptosis sensitivity, we noted an interesting observation indicating that Tg6/λ-MYC tumor cells in the bone marrow were resistant to rapamycin treatment when compared to tumor cells in the spleen (Figure 4). Rapamycin has been previously shown to induce apoptosis of cancer cells (33,34). It has also been shown to inhibit apoptosis in human promyelocytic leukemia cell line HL-60, which may be through rapamycin-induced down-regulation of FKBP12, rapamycin's binding partner (35). The resistance of Tg6/λ-MYC tumor cells to rapamycin may be related to factors present in the tumor microenvironment such as cytokines or tumor stromal cells (36,37). Quiescent leukemic stem cells residing in the bone marrow have been shown to be resistant to the treatment and this resistance can be broken if the cells are driven into the cell cycle (38). The low percent of CD19 positive bone marrow cells in our model may be non-cycling tumor stem cells and therefore resistant to the induction of apoptosis by rapamycin whereas tumor cells present in the spleen may have a more activated phenotype and as such be more susceptible to rapamycin. In addition, LMP2A has been shown to inhibit apoptosis induced by B cell receptor and TGF-β (24,39) and signaling through these receptors in different microenvironments may also play a role in the differential sensitivity of Tg6/λ-MYC tumor cells compared to λ-MYC tumor cells.

In line with our studies, there have been some reports suggesting that rapamycin can inhibit EBV-related PTLD (28,33), while others have indicated insufficiency of rapamycin monotherapy in the prevention of PTLD(34,40). This discrepancy may be related to differences in cellular and viral genes expressed but more importantly may be due to the evolution of the PTLD and the ability of cells to overcome rapamycin inhibition. In addition to inhibiting mTOR, rapamycin also inhibits the inhibitory feedback loop on the Akt activation (41). While mTORC1 complex is sensitive, the mTORC2 complex is resistant to rapamycin inhibition (42,43) and the activity of mTORC2 has been shown to be required for prostate tumor development (44). Even in the presence of rapamycin, the resistant mTORC2 complex is able to activate Akt leading to an incomplete inhibition of the PI3K/Akt/mTOR survival pathway (42,43,45,46) resulting in tumor cells addicted to Akt activation. Previous studies have shown that LMP2A activates the PI3K/Akt/mTOR pathway (22,23,25).

Therefore, more potent dual inhibitors of PI3K/Akt/mTOR pathway, such as BEZ235, p242, or Torin-1 may be more effective in inhibiting the lymphomas that occur in the Tg6/λ-MYC as was recently shown for KSHV tumor cells (36,47-50).

We demonstrate that rapamycin effectively and specifically reverses the LMP2A-induced splenomegaly and significantly impairs the development of tumors expressing LMP2A. Our data support previous studies that LMP2A modulates the PI3K/Akt/mTOR pathway and that this modulation is sensitive to mTOR inhibition. Furthermore, our data indicate that rapamycin could be a valuable candidate for the development of a treatment regimen for LMP2A-expressing EBV positive abnormalities LMP2A is thought to be expressed in most EBV-associated pathologies that occur in the human host, but the level of LMP2A expression can vary in the diverse disorders which include Burkitt's lymphoma, Hodgkin's lymphoma, nasopharyngeal carcinoma, HIV-associated secondary malignancies, and PTLD. How levels of LMP2A expression may impact the sensitivity of EBV-related pathologies to treatment with therapeutic agents such as rapamycin will need to be investigated. LMP2A transgenic mice with varying levels of LMP2A expression may offer an important experimental system to investigate this question.

Acknowledgments

R.L. is John Edward Porter Professor in Biomedical Research and supported by the Public Health Service grants R01 CA133063 and R01 CA073507 from the National Cancer Institute. We would like to thank members of the Longnecker laboratory for help in the completion of these studies. This work was also supported by the Northwestern University Interdepartmental ImmunoBiology Flow Cytometry Core Facility.

Financial Support: R.L. is John Edward Porter Professor in Biomedical Research and supported by the Public Health Service grants R01 CA133063 and R01 CA073507 from the National Cancer Institute.

List of Abbreviations

EBV	Epstein-Barr virus
LMP2A	EBV encoded latent membrane protein 2A
Tg6	transgenic mice expressing LMP2A
λ-MYC	transgenic mice expressing MYC under the regulatory DNA sequence of immunoglobulin λ gene
mTOR	mammalian target of rapamycin
BCR	B cell receptor
Rag1 KO	recombinase activating gene-1 knockout mice
PTLD	post-transplant lymphoproliferative disorders

References

1. Rickinson, AB.; Kieff, E. Epstein-Barr Virus. In: Knipe, DM.; H, PT.; G, DE., et al., editors. Fields Virology. 5 ed.. Lippincott Williams & Wilkins; Philadelphia: 2007. p. 2655-700.
2. Thorley-Lawson DA, Gross A. Persistence of the Epstein-Barr virus and the origins of associated lymphomas. N Engl J Med. 2004; 350:1328–37. [PubMed: 15044644]
3. Merchant M, Caldwell RG, Longnecker R. The LMP2A ITAM is essential for providing B cells with development and survival signals in vivo. J Virol. 2000; 74:9115–24. [PubMed: 10982358]
4. Bieging KT, Swanson-Mungerson M, Amick AC, Longnecker R. Epstein-Barr virus in Burkitt's lymphoma: a role for latent membrane protein 2A. Cell Cycle. 2010; 9:901–8. [PubMed: 20160479]

5. Caldwell RG, Wilson JB, Anderson SJ, Longnecker R. Epstein-Barr virus LMP2A drives B cell development and survival in the absence of normal B cell receptor signals. Immunity. 1998; 9:405–11. [PubMed: 9768760]
6. Longnecker R, Merchant M, Brown ME, Fruehling S, Bickford JO, Ikeda M, et al. WW- and SH3-domain interactions with Epstein-Barr virus LMP2A. Exp Cell Res. 2000; 257:332–40. [PubMed: 10837147]
7. Ikeda M, Ikeda A, Longnecker R. Lysine-independent ubiquitination of Epstein-Barr virus LMP2A. Virology. 2002; 300:153–9. [PubMed: 12202215]
8. Ikeda M, Longnecker R. The c-Cbl proto-oncoprotein downregulates EBV LMP2A signaling. Virology. 2009; 385:183–91. [PubMed: 19081591]
9. Winberg G, Matskova L, Chen F, Plant P, Rotin D, Gish G, et al. Latent membrane protein 2A of Epstein-Barr virus binds WW domain E3 protein-ubiquitin ligases that ubiquitinate B-cell tyrosine kinases. Mol Cell Biol. 2000; 20:8526–35. [PubMed: 11046148]
10. Fruehling S, Longnecker R. The immunoreceptor tyrosine-based activation motif of Epstein-Barr virus LMP2A is essential for blocking BCR-mediated signal transduction. Virology. 1997; 235:241–51. [PubMed: 9281504]
11. Fruehling S, Swart R, Dolwick KM, Kremmer E, Longnecker R. Tyrosine 112 of latent membrane protein 2A is essential for protein tyrosine kinase loading and regulation of Epstein-Barr virus latency. J Virol. 1998; 72:7796–806. [PubMed: 9733815]
12. Bell AI, Groves K, Kelly GL, Croom-Carter D, Hui E, Chan AT, et al. Analysis of Epstein-Barr virus latent gene expression in endemic Burkitt's lymphoma and nasopharyngeal carcinoma tumour cells by using quantitative real-time PCR assays. J Gen Virol. 2006; 87:2885–90. [PubMed: 16963746]
13. Xue SA, Labrecque LG, Lu QL, Ong SK, Lampert IA, Kazembe P, et al. Promiscuous expression of Epstein-Barr virus genes in Burkitt's lymphoma from the central African country Malawi. Int J Cancer. 2002; 99:635–43. [PubMed: 12115495]
14. Ong KW, Teo M, Lee V, Ong D, Lee A, Tan CS, et al. Expression of EBV latent antigens, mammalian target of rapamycin, and tumor suppression genes in EBV-positive smooth muscle tumors: clinical and therapeutic implications. Clin Cancer Res. 2009; 15:5350–8. [PubMed: 19706821]
15. Tao Q, Robertson KD, Manns A, Hildesheim A, Ambinder RF. Epstein-Barr virus (EBV) in endemic Burkitt's lymphoma: molecular analysis of primary tumor tissue. Blood. 1998; 91:1373–81. [PubMed: 9454768]
16. Magrath I. The pathogenesis of Burkitt's lymphoma. Adv Cancer Res. 1990; 55:133–270. [PubMed: 2166998]
17. Kovalchuk AL, Qi CF, Torrey TA, Taddesse-Heath L, Feigenbaum L, Park SS, et al. Burkitt lymphoma in the mouse. J Exp Med. 2000; 192:1183–90. [PubMed: 11034608]
18. Adams JM, Harris AW, Pinkert CA, Corcoran LM, Alexander WS, Cory S, et al. The c-myc oncogene driven by immunoglobulin enhancers induces lymphoid malignancy in transgenic mice. Nature. 1985; 318:533–8. [PubMed: 3906410]
19. Bieging KT, Amick AC, Longnecker R. Epstein-Barr virus LMP2A bypasses p53 inactivation in a MYC model of lymphomagenesis. Proc Natl Acad Sci U S A. 2009; 106:17945–50. [PubMed: 19815507]
20. Bultema R, Longnecker R, Swanson-Mungerson M. Epstein-Barr virus LMP2A accelerates MYC-induced lymphomagenesis. Oncogene. 2009; 28:1471–6. [PubMed: 19182823]
21. Krams SM, Martinez OM. Epstein-Barr virus, rapamycin, and host immune responses. Curr Opin Organ Transplant. 2008; 13:563–8. [PubMed: 19060543]
22. Fukuda M, Longnecker R. Epstein-Barr virus latent membrane protein 2A mediates transformation through constitutive activation of the Ras/PI3-K/Akt Pathway. J Virol. 2007; 81:9299–306. [PubMed: 17582000]
23. Portis T, Longnecker R. Epstein-Barr virus (EBV) LMP2A mediates B-lymphocyte survival through constitutive activation of the Ras/PI3K/Akt pathway. Oncogene. 2004; 23:8619–28. [PubMed: 15361852]

24. Fukuda M, Longnecker R. Latent membrane protein 2A inhibits transforming growth factor-beta 1-induced apoptosis through the phosphatidylinositol 3-kinase/Akt pathway. J Virol. 2004; 78:1697–705. [PubMed: 14747535]
25. Swart R, Ruf IK, Sample J, Longnecker R. Latent membrane protein 2A-mediated effects on the phosphatidylinositol 3-Kinase/Akt pathway. J Virol. 2000; 74:10838–45. [PubMed: 11044134]
26. Morrison JA, Klingelhutz AJ, Raab-Traub N. Epstein-Barr virus latent membrane protein 2A activates beta-catenin signaling in epithelial cells. J Virol. 2003; 77:12276–84. [PubMed: 14581564]
27. Moody CA, Scott RS, Amirghahari N, Nathan CO, Young LS, Dawson CW, et al. Modulation of the cell growth regulator mTOR by Epstein-Barr virus-encoded LMP2A. J Virol. 2005; 79:5499–506. [PubMed: 15827164]
28. Vaysberg M, Balatoni CE, Nepomuceno RR, Krams SM, Martinez OM. Rapamycin inhibits proliferation of Epstein-Barr virus-positive B-cell lymphomas through modulation of cell-cycle protein expression. Transplantation. 2007; 83:1114–21. [PubMed: 17452903]
29. Caldwell RG, Brown RC, Longnecker R. Epstein-Barr virus LMP2A-induced B-cell survival in two unique classes of EmuLMP2A transgenic mice. J Virol. 2000; 74:1101–13. [PubMed: 10627520]
30. Wendel HG, Malina A, Zhao Z, Zender L, Kogan SC, Cordon-Cardo C, et al. Determinants of sensitivity and resistance to rapamycin-chemotherapy drug combinations in vivo. Cancer Res. 2006; 66:7639–46. [PubMed: 16885364]
31. Mombaerts P, Iacomini J, Johnson RS, Herrup K, Tonegawa S, Papaioannou VE. RAG-1-deficient mice have no mature B and T lymphocytes. Cell. 1992; 68:869–77. [PubMed: 1547488]
32. Jones RJ, Chen Q, Voorhees PM, Young KH, Bruey-Sedano N, Yang D, et al. Inhibition of the p53 E3 ligase HDM-2 induces apoptosis and DNA damage--independent p53 phosphorylation in mantle cell lymphoma. Clin Cancer Res. 2008; 14:5416–25. [PubMed: 18765533]
33. Nepomuceno RR, Balatoni CE, Natkunam Y, Snow AL, Krams SM, Martinez OM. Rapamycin inhibits the interleukin 10 signal transduction pathway and the growth of Epstein Barr virus B-cell lymphomas. Cancer Res. 2003; 63:4472–80. [PubMed: 12907620]
34. Ishizuka T, Sakata N, Johnson GL, Gelfand EW, Terada N. Rapamycin potentiates dexamethasone-induced apoptosis and inhibits JNK activity in lymphoblastoid cells. Biochem Biophys Res Commun. 1997; 230:386–91. [PubMed: 9016789]
35. Johnson KL, Lawen A. Rapamycin inhibits didemnin B-induced apoptosis in human HL-60 cells: evidence for the possible involvement of FK506-binding protein 25. Immunol Cell Biol. 1999; 77:242–8. [PubMed: 10361256]
36. Bhatt AP, Bhende PM, Sin SH, Roy D, Dittmer DP, Damania B. Dual inhibition of PI3K and mTOR inhibits autocrine and paracrine proliferative loops in PI3K/Akt/mTOR-addicted lymphomas. Blood. 2010
37. Dierks C, Grbic J, Zirlik K, Beigi R, Englund NP, Guo GR, et al. Essential role of stromally induced hedgehog signaling in B-cell malignancies. Nat Med. 2007; 13:944–51. [PubMed: 17632527]
38. Saito Y, Uchida N, Tanaka S, Suzuki N, Tomizawa-Murasawa M, Sone A, et al. Induction of cell cycle entry eliminates human leukemia stem cells in a mouse model of AML. Nat Biotechnol. 2010; 28:275–80. [PubMed: 20160717]
39. Fukuda M, Longnecker R. Epstein-Barr virus (EBV) latent membrane protein 2A regulates B-cell receptor-induced apoptosis and EBV reactivation through tyrosine phosphorylation. J Virol. 2005; 79:8655–60. [PubMed: 15956608]
40. Holtan SG, Porrata LF, Colgan JP, Zent CS, Habermann TM, Markovic SN. mTOR inhibitor monotherapy is insufficient to suppress viremia and disease progression in Epstein-Barr virus-driven lymphoproliferative disorders (EBV-LPD). Am J Hematol. 2008; 83:688–9. [PubMed: 18528858]
41. Sun SY, Rosenberg LM, Wang X, Zhou Z, Yue P, Fu H, et al. Activation of Akt and eIF4E survival pathways by rapamycin-mediated mammalian target of rapamycin inhibition. Cancer Res. 2005; 65:7052–8. [PubMed: 16103051]

42. Sarbassov DD, Guertin DA, Ali SM, Sabatini DM. Phosphorylation and regulation of Akt/PKB by the rictor-mTOR complex. Science. 2005; 307:1098–101. [PubMed: 15718470]
43. Sarbassov DD, Ali SM, Kim DH, Guertin DA, Latek RR, Erdjument-Bromage H, et al. Rictor, a novel binding partner of mTOR, defines a rapamycin-insensitive and raptor-independent pathway that regulates the cytoskeleton. Curr Biol. 2004; 14:1296–302. [PubMed: 15268862]
44. Guertin DA, Stevens DM, Saitoh M, Kinkel S, Crosby K, Sheen JH, et al. mTOR complex 2 is required for the development of prostate cancer induced by Pten loss in mice. Cancer Cell. 2009; 15:148–59. [PubMed: 19185849]
45. Jacinto E, Loewith R, Schmidt A, Lin S, Ruegg MA, Hall A, et al. Mammalian TOR complex 2 controls the actin cytoskeleton and is rapamycin insensitive. Nat Cell Biol. 2004; 6:1122–8. [PubMed: 15467718]
46. Guertin DA, Sabatini DM. An expanding role for mTOR in cancer. Trends Mol Med. 2005; 11:353–61. [PubMed: 16002336]
47. Hsieh AC, Costa M, Zollo O, Davis C, Feldman ME, Testa JR, et al. Genetic dissection of the oncogenic mTOR pathway reveals druggable addiction to translational control via 4EBP-eIF4E. Cancer Cell. 2010; 17:249–61. [PubMed: 20227039]
48. Feldman ME, Apsel B, Uotila A, Loewith R, Knight ZA, Ruggero D, et al. Active-site inhibitors of mTOR target rapamycin-resistant outputs of mTORC1 and mTORC2. PLoS Biol. 2009; 7:e38. [PubMed: 19209957]
49. Serra V, Markman B, Scaltriti M, Eichhorn PJ, Valero V, Guzman M, et al. NVP-BEZ235, a dual PI3K/mTOR inhibitor, prevents PI3K signaling and inhibits the growth of cancer cells with activating PI3K mutations. Cancer Res. 2008; 68:8022–30. [PubMed: 18829560]
50. Thoreen CC, Kang SA, Chang JW, Liu Q, Zhang J, Gao Y, et al. An ATP-competitive mammalian target of rapamycin inhibitor reveals rapamycin-resistant functions of mTORC1. J Biol Chem. 2009; 284:8023–32. [PubMed: 19150980]

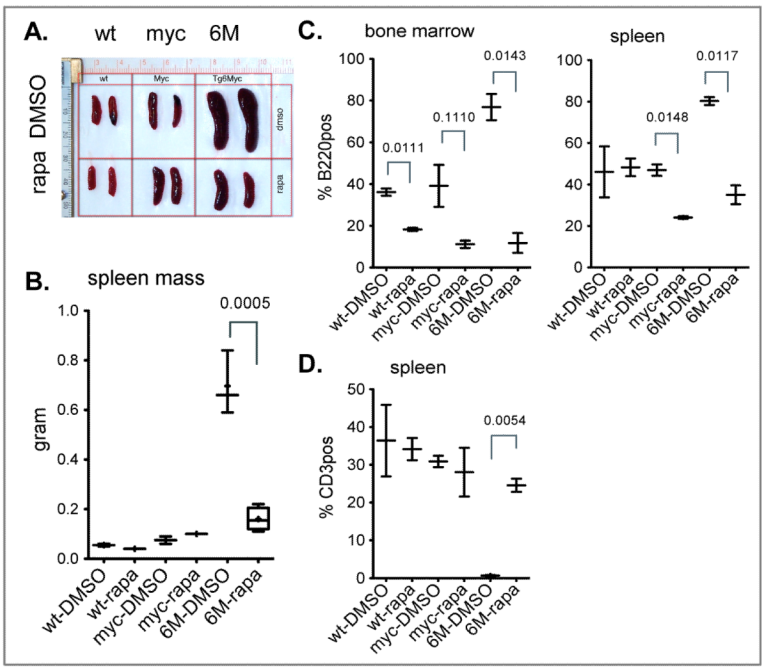

Figure 1. Rapamycin reverses splenomegaly in Tg6/λ-MYC mice

Wild type (wt), λ-MYC (myc), or Tg6/λ-MYC (6M) mice were treated daily with 5-mg/kg rapamycin (rapa) or DMSO for 10 days and analyzed on day 11. The spleens of respective mice from one of two experiments are depicted (A). The weight of the spleens in each group is graphed in box-and-whisker format (B). The percentages of B220 positive cells in bone marrow (C, left panel) and in spleen (C, right panel) as well as the percentage of CD3 positive splenocytes (D) in respective groups are shown. Each data point is from 2-6 mice. The box for each group represents the interquartile range (25-75 percentiles) and the longer horizontal line in the box represents the median value. The mean is marked as + sign, which is a short horizontal line when it coincides with a vertical line or absent when the median and mean correspond. The whiskers indicate minimum and maximum data points. When there are fewer than four data points in a group, a vertical line is shown instead of a box. The numbers above the given connected data points indicate p values.

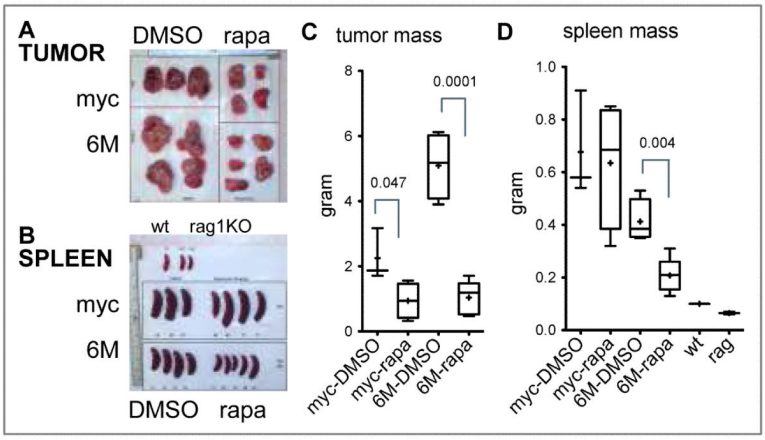

Figure 2. Rapamycin inhibits tumor growth and splenomegaly in Rag1 KO mice that have been implanted with Tg6/λ-MYC lymphoma cells

Data from one of two experiments are shown. Shown are tumors (A) and spleens (B) collected form the Rag1 KO mice that had been implanted with Tg6/λ-MYC (6M) or λ-MYC (myc) lymphoma cells and then treated with either rapamycin (rapa) or DMSO. The representative spleens from one wild type and two Rag1 KO naive mice are also shown as reference in B (on the top) and D. The weight of tumors (C) and spleens (D) from respective groups are graphed as in Figure 1.

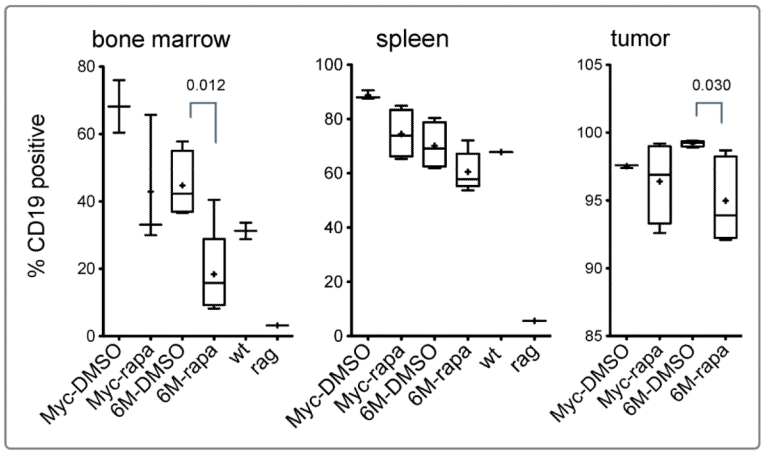

Figure 3. Rapamycin decreases metastasis of Tg6/λ-MYC tumor cells into bone marrow

The percentage of CD19 positive cells, sequentially gated on 7AAD-negative (live), singlet, lymphocyte, and CD19, as assessed with flow cytometry from bone marrow (left panel), spleen (middle panel), or tumor cells (right panel) obtained from the groups in Figure 2. Shown are also the percentages of CD19 positive cells in bone marrow and spleen from naïve wild type and Rag1 KO mice. The data are graphed as in Figure 1.

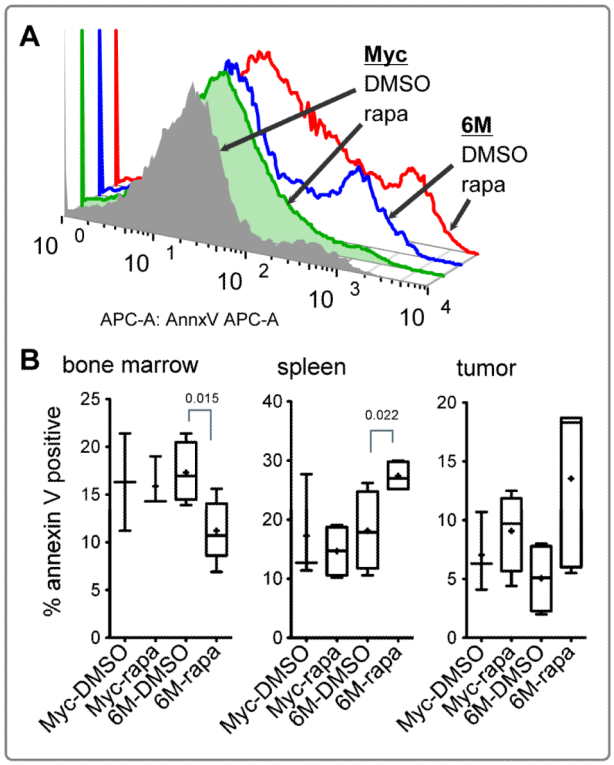

Figure 4. Rapamycin induces apoptosis in LMP2A positive lymphoma cells

Representative flow plots (A) showing annexin V staining of 7AAD-negative (live) tumor cells from groups in Figure 2. The percentage of the annexin V positive cells (B) sequentially gated on 7AAD-negative, singlet, lymphocyte, and CD19 positive cells from bone marrow (left panel), spleen (middle panel), or tumor cells (right panel). The data are graphed as in Figure 1.